Water Current Velocity Measurements by a Magnetometer-based Tilt

Juan Montiel-Caminos, Nieves G. Hernandez-Gonzalez, Javier Sosa and Juan A. Montiel-Nelson
Institute for Applied Microelectronics
University of Las Palmas de Gran Canaria
Las Palmas de Gran Canaria, Spain
ORCID: 0000-0001-5156-7646, 0000-0002-2401-4461, 0000-0003-1838-3073, 0000-0003-4323-8097

2024 IEEE 67th International Midwest Symposium on Circuits and Systems (MWSCAS) | 979-8-3503-8717-9/24/$31.00 ©2024 IEEE | DOI: 10.1109/MWSCAS60917.2024.10658690

***Abstract*—A novel instrument based on the tilt-drag principle is developed for measuring the instantaneous velocity of the water current. Instead to obtain the tilt by an accelerometer, a magnetometer is used. For a range of underwater velocities from 5 cm/s to 50 cm/s, the resolution of the instrument is 8.5 bits. The water velocity is obtained using edge computation by a microcontroller with a core based on an ARM CORTEX M0+. The error is less than a 5% and the sensitivity 0.12 $cm/s/LSB$**

***Index Terms*—water current meter, edge computing, sensor-network**

I. Introduction

Nowadays, it is well known that the use of coastal zones defines multiple economic and social challenges. The deployment of new economic activities in already exploited territories, such as the tourism industry or compliance with new environmental legislation, requires particular approaches. An example of this is the economy of the Canary Islands in Spain, originally oriented towards tourism exploitation, is now shifting towards renewable energy and aquaculture industries. In both cases, the deployment of non-tourist activities is relegated to off-shore coastal areas.

These activities impact marine biodiversity, particularly in mesophotic habitats (30-150 m depth) [1], [2]. In this sense, in most cases it is mandatory to study the environmental parameters of the deployment location in terms of turbidity, temperature and water velocity, among others [3].

Of all these measures, the one that requires the greatest computational and therefore energy expenditure is the profiling of marine currents [4]. There are two solutions that achieve similar precision: those based on Doppler or those based on the drag-tilt principle [5]. However, instruments based on the tilt-drag principle require less computational effort and present a low cost compared to other solutions [6]. In this work, a novel water current profiler for long-term ocean currents characterization in deep and offshore waters is presented.

The proposed profiler is a system of systems, which allows acquiring long- and short-term water current velocity measurements. It is built replicating a unique module. Each module is an embedded system stacked on top of other identical module that connects to a WAN port on a buoy on the sea surface. In addition, each module incorporates an intelligent algorithm [7] based on neural networks which compute the fundamental frequencies onboard.

The measurement made use the drag-tilt principle. In common words, an arm anchored to a pivot point with a bob at its other end changes its inclination depending on gravity, buoyancy, and the buoyant force of water. In particular, water current velocities are obtained by the relationship between drag force $\vec{F_D}$, hydrostatic buoyancy $\vec{F_B}$, and gravitational force $\vec{F_g}$ (see Fig. 1).

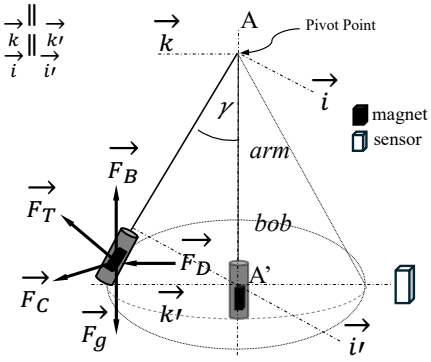

Fig. 1: Principle of operation of the instrument.

If the measurement system is in equilibrium the sum of forces is zero. Otherwise, if the sum of forces is positive, the bob floats towards the surface of the water. When the result is negative, the bob stands towards the seabed. The inclination γ of the arm-bob of the mechanical system is related to the drag force $\vec{F_D}$, and this in turn to the fluid velocity. This is the so called drag-tilt principle.

The literature and industrial solutions uses an accelerometer located in the bob measuring the tilt. The main problem of those approaches is the wiring between the bob and the entire water current profiler system. To solve this wiring problem, this research proposes to move the electronics of the bob to a fixed location of the measurement module and place a magnet on the bob.

In this work, each measurement module includes an embedded system based on an ARM CORTEX M0+ ultra-low-power microcontroller. Also, we use as magnetometer the FXOS8700CQ acquisition subsystem from NXP to measures the magnetic in three orthogonal axes. Its sensitivity is 0.1 $\mu T/LSB$, for the magnetic range of $\pm$ 1200 μT and 14-bits of resolution.

The neodymium magnet, used as magnetic field generator, is attached to the bob. By this approach, we remove the wiring of power supplying and digital data communications of the bob. The arm plus the bob has a length of 76 mm. The arm is made of Acrylonitrile Butadiene Styrene (ABS) High Impact plastic. In terms of drag, the volume of the arm is negligible compared to the volume of the bob.

In this research, a magnetic displacement coming from two different sources is considered. One is the Earth's natural magnetic field and also the misalignment between the components of the measurement system (magnet/bob and magnetometer). Once the complete system is deployed, this value is obtained and considered constant throughout the measurements as long as the placement of the complete system is not modified.

For each measurement, the resulting tilt for a drag force due to current velocities in the range of 5-50 cm/s are obtained with a resolution of 8.5 bits. The spatial range of the proposed magnetic-based tilt meter is ≈ 0.6 rad., i.e, the solid angle γ of the arm is close to 34°.

The paper is organized as follows. Section II describes the fundamentals and theoretical principle of the instrument. It is demonstrated theoretically how to obtain the fluid velocity from the inclination of a magnet by measuring the magnetic field produced by the neodymium magnet. Section III illustrates the details of the prototype, and introduces the governing equations and the Onboard Computational Unit for edge computing. Section IV provides measurement results for the offset, measure range and resolution of the proposed magnetic-tilt system and the edge-computation of the fluid-velocity values $\|\vec{u}\|$. Finally, conclusions are presented in Section V.

II. Fundamentals of Instrument based on Magnetic field

In this work, it is proposed the design and implementation of an instrument to determine the profile of water velocities based on a magnetometer. Based on the drag-tilt principle, drag force $\vec{F_D}$ is produced by a water flow. In other words, the tilt angle is a function of the water velocity. Based on Fig. 1, if the arm-bob is on the A-A' axis, $\vec{F}_D$ pushing the bob is zero.

The forces of gravity $\vec{F}_g$ and buoyancy $\vec{F}_B$ are considered, because the instrument is submerged:

$$\vec{F}_g = m \times \vec{g}, \quad \text{and} \tag{1}$$

$$\vec{F}_B = \rho \times \vec{g} \times V, \tag{2}$$

where V is the volume of the bob. In equilibrium, the tension force $\vec{T_{arm}}$ supported by the arm is:

$$\vec{T}_{arm} = \vec{F}_g - \vec{F}_B = \vec{g} \times (m - \rho \times V) \tag{3}$$

The system of forces outside the equilibrium position is defined by $\vec{F}_T + \vec{F}_C = \vec{F}_D + \vec{F}_G$, where $\vec{F}_T$ and $\vec{F}_C$ are the tangential and the centripetal forces respectively. $\vec{F}_G$ is the difference between the buoyancy force $\vec{F}_B$ and the gravity force $\vec{F}_g$.

A. Magnetic Bob

The bob is an encapsulated neodymium magnet N52. Its size is 3 mm x 3 mm x 3 mm. The objective is to determine the drag force as a function of the tilt angle by using its magnetic field. If the bob is located out its equilibrium, the magnetic field changes (see Fig: 2a).

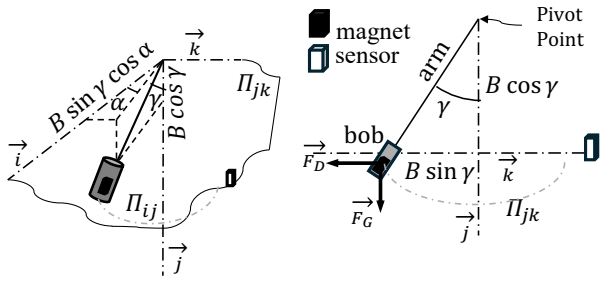

(a) (b)

Fig. 2: (**a**) Tilt angles out of equilibrium position. (**b**) Decomposition of the system of forces at the plane π_{jk}.

The magnetic field produced by the encapsulated magnet is defined in the equations:

$$\vec{M}_i = B\sin(\gamma)\cos(\alpha)\vec{i} \tag{4}$$

$$\vec{M}_j = B\cos(\gamma)\vec{j} \tag{5}$$

$$\vec{M}_k = B\sin(\gamma)\sin(\alpha)\vec{k} \tag{6}$$

Using these equations, the relationship between the magnetic field and the tilt angle of the arm-bob element is obtained.

On the other hand, the drag force depends on three constants C_d, A, ρ and the vector $\vec{u}$. C_d is the drag coefficient, it is related to the shape and material of the bob. A is the area of the object facing the fluid. ρ is the density of the fluid, particularly that of salt water and $\vec{u}$ its velocity. In this scenario, the drag Force is defined by

$$\|\vec{F}_D\| = \frac{1}{2} C_d A \rho u^2 \tag{7}$$

From the plane Π_{jk}, it is obtained the relationship between the drag force, the tilt angle, and the magnetic field (see Fig.2b).

$$\|\vec{F}_D\| \approx B\sin(\gamma)\ ; \|\vec{F}_D\|\cos(\gamma) = \|\vec{F}_G\| \approx mg\sin(\gamma) \tag{8}$$

Finally, combining (7) and (8), the velocity of the fluid u is defined as:

$$u^2 = 2\frac{mg}{\rho C_d A}\frac{\sin(\gamma)}{\cos(\gamma)} = k\tan(\gamma), \tag{9}$$

where, k is a scale factor that depends on m, g, ρ, C_d and A. Based on Fig.2a, the relationship between the magnetic field generated by the magnet and the tilt angle of the sensor node is:

$$\|\vec{M}_k + \vec{M}_i\| = B\sin(\gamma) \tag{10}$$

Then, from (10) and (6), the relation between the magnetic field and the tilt angle is:

$$\frac{\|\vec{M}_k + \vec{M}_i\|}{\|\vec{M}_j\|} = \tan(\gamma) \tag{11}$$

Finally, the magnitude of the water velocity is obtained from (9), (11), and (12) as:

$$u^2 = 2\frac{mg}{\rho C d A}\frac{\|\vec{M}_k + \vec{M}_i\|}{\|\vec{M}_j\|} \tag{12}$$

III. Prototype Desing

A. Sensor node

The neodymium magnet N52 is encapsulated in a Polymethyl Methacrylate (PMMA) cylinder. The bob has a weight of 0.2 kg of 6.35 mm diameter and 25.2 mm length. Finally, the fluid velocity in relation to the magnetic field of the sensor node is defined by:

$$u^2 = \pi\frac{\rho_{bob}}{\rho} g \frac{\phi}{C_d}\frac{\|\vec{M}_k + \vec{M}_i\|}{\|\vec{M}_j\|} \mid \rho_{bob} = \frac{m_{pac} + m_{mag}}{V_{pac}} \tag{13}$$

where ρ_{bob}/ρ is the density ratio, ϕ the bob cylinder diameter, C_d drag coefficient, and g the gravity constant. m_{pac} and m_{mag} are the PMMA and magnet masses, respectively.

B. Onboard Computational Unit

The Onboard Computational Unit (OCU) is based on an ultra-low power ARM Cortex-M0+, with 512 KB of flash memory (MKL28Z512VLL7 from NXP). It also includes a triaxial magnetometer (FXOS8700CQ) with 16-bit resolution. The OCU operates in stand-alone mode because it is designed to be powered by batteries. The goal is to integrate the OCU into an underwater sensor network [6]. The integrated intelligence (edge computing) and ultra-low power consumption operation allow long-term (>180 days) measuring and characterizing the water velocities in offshore areas at mesophotic depths [7]. The instrument records data over long time periods to create an oceanographic atlas that includes the water velocity measures.

On the other hand, the orthogonality of the axes is guaranteed by the design of the IC. However, misalignment between the IC and the designed structure must be considered. This is an offset error and is mitigated by measuring the misalignment error for each OCU. In addition, the relationship between power consumption and sample rate is linear. As the sampling rate increases, so does the power consumption. The sampling rate is 12.5 samples per second. This frequency allows to measure locally the tidal currents [5].

C. Onboard Laboratory System

The vertical spatial resolution of the instrument is 10 cm. The Onboard Laboratory system (OBLS) is a linear array of currents meters built by stacking 10 OCUs vertically (see Fig.3b). The structure that makes up the instrument is called OBLS. It allows the recording data, computing the velocities and transmit the result. The battery operation allows

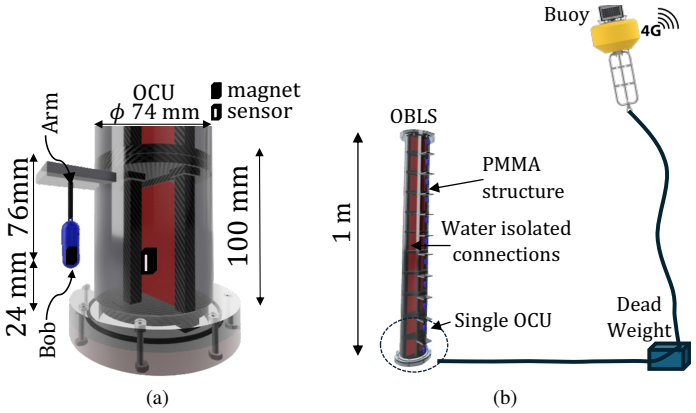

Fig. 3: Designed module and water current meter: (**a**) single Onboard Computational Unit (OCU) and stacked structure (**b**) Onboard Laboratory System (OBLS).

to measure continuously at least 6 months. Data transmission is carried out through a wired system for communicating the measurements from the OBLS to land using a buoy. The buoy has a $4G$ communication module with the coast. The system stores the data locally on a memory card and also transmits it to Internet Cloud Servers.

The system is reconfigurable through its online connection. That is, the sampling frequency among other parameters can be modified. The buoy works with an internal battery. And it is rechargeable with a small solar panel. The buoy also has a datalogger with GPS.

IV. Experiments

Because the relative position of the magnetic-bob in relation to the onboard magnetometer, the spatial offset should be measured. Spatial offset is obtained experimentally by static magnetic field measurements. The bob is placed at different positions, and the magnetic field ($\vec{M}_i$, $\vec{M}_j$, $\vec{M}_k$) is obtained by the onboard magnetometer FXOS8700CQ. A rectangular prism of 50 mm x 30 mm x 30 mm is scanned with a spatial resolution of 1 mm. And therefore, as described in section III-B, a magnetic field analysis was performed to determine the position of the components. Fig.4 illustrates the measurements obtained for the rectangular prism. Note that the magnetometer is not centered. This is because the magnetometer FXOS8700CQ is not placed, symmetrically, on the OCU, i.e., this deviation, that was obtained during the calibration phase of the instrument, provides the offset with respect the center of the IC FXOS8700CQ. From these data, we obtain the spatial offset.

Fig. 5 illustrates the measured magnetic modules ($\|\vec{M}_i\|$, $\|\vec{M}_j\|$, $\|\vec{M}_k\|$, and $\|\vec{M}\|$). Note that the trajectory of magnetic-bob attached to the arm follows a spherical dome. The measured magnetic field and module were obtaining for a magnetic-bob attached to a rigid arm with a pivotal point at 76 mm from the base of the OCU (see Fig. 3a). The spatial offset was considered for the magnetic field measurements.

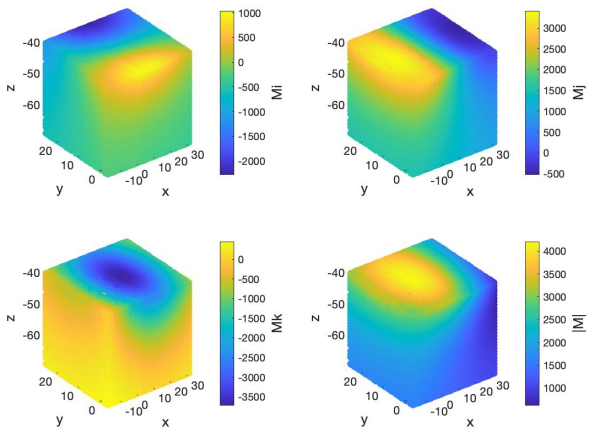

Fig. 4: Magnetic field misalignment analysis of the instrument.

The spherical dome has a solid angle of $\approx 0.6\ rad.$, i.e., the angle γ (see Fig. 1) of the arm is close to 34°. This solid angle corresponds to the maximum current velocity of 50 cm/s. Fig. 6 presents the velocity of the fluid $\vec{u}$ in terms of the magnetic field components $\|\vec{M}_i\|$, $\|\vec{M}_j\|$, and $\|\vec{M}_k\|$. For simplicity, this figure is obtained when the velocity fluid is oriented perpendicular to the magnetometer IC, i.e., the axial component $\vec{M}_k$ is zero. The worst case rounding error is $\pm 1/2$ LSB. The final resolution for measured the square fluid velocity u^2 is 8 $1/2$ bits. In Fig. 6, the module of the water

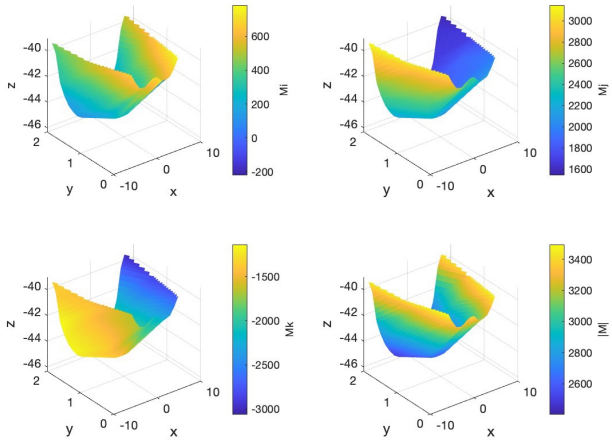

Fig. 5: Measured module of magnetic field for a magnetic attached to a rigid arm ($\|\vec{M}_i\|$, $\|\vec{M}_j\|$, $\|\vec{M}_k\|$ and $\|\vec{M}\|$).

velocity is in the range from 5 to 50 cm/s. The magnetic-bob is pushed by a drag-force which is perpendicular to the plane x-y, i.e., in the direction of z-axis. The x-axis is represented in terms of fullscale. That is, 100% and 0% mean 50 cm/s and 0.5 cms/s respectively. Fig. 6 d) is the edge computation of the $|\vec{M}_k + \vec{M}_i\|/\|\vec{M}_j\|$ for the measurements in solid line, whereas the dots are the values of the ratio water velocity and k. The difference between the solid line, edge-computed $\|\vec{M}_k + \vec{M}_i\|/\|\vec{M}_j\|$ and u/k is less than a 5%.

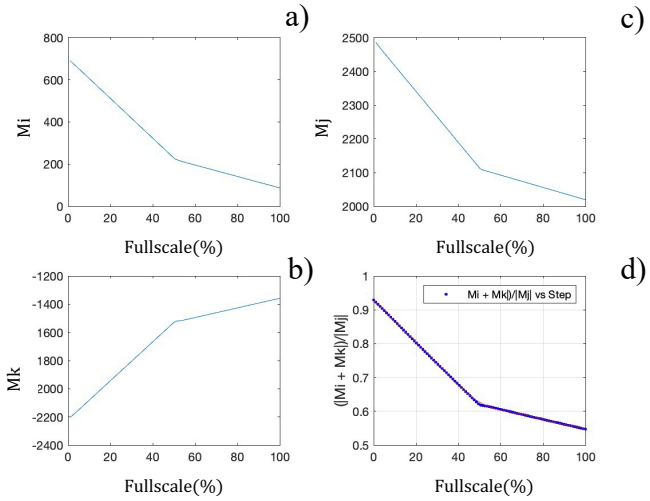

Fig. 6: Measured magnetic field values $\vec{M}i$ (a), $\vec{M}j$ (c) and $\vec{M}k$ (b), respectively for a water velocity of direction (0,0,-1) in relation to the magnetometer axis and (d) is u/k ratio.

V. Conclusions

A new magnetic-tilt current-meter is proposed in this work. The instrument use a magnet which is attached by a rigid massless arm to a pivotal point. The magnetometer FXOS8700CQ is connected to a microcontroller. The proposed magnetic-tilt measures the magnetic field of the N52 magnet with a sensitivity of 0.1 $\mu T/LSB$, for the magnetic range of $\pm 1200 \mu T$ and 14-bits. For measuring water velocities in the range of 5 cm/s to 50 cm/s, the magnetic field dynamic range is reduced to 9-bits. For obtaining the square of the water current velocity u^2, the instrument resolution is approaching to 8.5 bits, because the worst case rounding error for integer divisions. The advantage of a magnetic-tilt against accelerometer-tilt is the simplicity in the design of the arm-bob mechanical device.

Acknowledgment

This paper is part of the R+D+i projects PID2020-117251RB-C21, funded by MCIN/AEI/ 10.13039/501100011033/, and TED2021-131470B-100, funded by MCIN/AEI/10.13039/ 501100011033/ and by the European Union NextGenerationEU/ PRTR.

References

[1] Rocha, L.A.; Pinheiro, H.T.; Shepherd, B.; Papastamatiou, Y.P.; Luiz, O.J.; Pyle, R.L.; Bongaerts, P. Mesophotic coral ecosystems are threatened and ecologically distinct from shallow water reefs. Science 2018, 361, 281–284, doi:10.1126/science.aaq1614.

[2] Bongaerts, P.; Smith,T.B. Beyond the "deep reef refuge" hypothesis: a conceptual framework to characterize persistence at depth. In: Mesophotic Coral Ecosystems. Springer, Cham, 2019, pp. 881–895.

[3] Loya, Y.; Eyal, G.; Treibitz, T.; Lesser, M.P.; Appeldoorn, R. Theme section on mesophotic coral ecosystems: advances in knowledge and future perspectives. Coral Reefs 2016, 35, 1–9, doi:10.1007/s00338-016-1410- 7.

[4] Eyal, G.; Pinheiro, H.T. Mesophotic ecosystems: The link between shallow and deep-sea habitats. Diversity 2020, 12, 1–4, doi:10.3390/d12110411.
[5] Sosa, J.; Montiel-Nelson, J.-A. Novel Deep-Water Tidal Meter for Offshore Aquaculture Infrastructures. Sensors 2022, 22, 5513. doi: 10.3390/s22155513.
[6] Santana Sosa, G.; Santana Abril, J.; Sosa, J.; Montiel-Nelson, J.-A.; Bautista, T. Design of a Practical Underwater Sensor Network for Offshore Fish Farm Cages. Sensors 2020, 20, 4459. doi: 10.3390/s20164459.
[7] Hernandez-Gonzalez, N.G.; Montiel-Caminos, J.; Sosa, J.; Montiel-Nelson, J.A. An Edge Computing Application of Fundamental Frequency Extraction for Ocean Currents and Waves. Sensors 2024, 24, 1358. https://doi.org/10.3390/s24051358
[8] Lewis, M.; Neill, S.P.; Robins, P.; Hashemi, M.R.; Ward, S. Characteristics of the velocity profile at tidal-stream energy sites. *Renew. Energy* 2017, *114*, 258–272. https://doi.org/10.1016/j.renene.2017.03.096.luego
[9] Zhang, X.; Simons, R.; Zheng, J.; Zhang, C. A review of the state of research on wave-current interaction in nearshore areas. *Ocean. Eng.* 2022, *243*, https://doi.org/10.1016/j.oceaneng.2021.110202.